Neutral Amino Acid Transporter ASCT1 Is Preferentially Expressed in L-Ser-Synthetic/Storing Glial Cells in the Mouse Brain with Transient Expression in Developing Capillaries

Kazuhisa Sakai,[1,2]* Hidemi Shimizu,[1]* Tatsuro Koike,[2] Shigeki Furuya,[3] and Masahiko Watanabe[1]

[1]Department of Anatomy, Hokkaido University School of Medicine, Sapporo 060-8638, Japan, [2]Molecular Neurobiology Laboratory, Hokkaido University Graduate School of Science, Sapporo 060-0810, Japan, and [3]Neuronal Circuit Mechanisms Research Group, The Institute of Physical and Chemical Research (RIKEN) Brain Science Institute, Wako, Saitama 351-0198, Japan

Nonessential amino acid L-Ser plays an essential role in neuronal survival and differentiation, through preferential expression of the L-Ser biosynthetic enzyme 3-phosphoglycerate dehydrogenase (3PGDH), in particular in glial cells but not in neurons. To seek the molecular candidates responsible for glia-borne L-Ser transport, we performed histochemical analyses on amino acid transporter ASCT1, which prefers small neutral amino acids, such as Ala, Ser, Cys, and Thr, and mediates their obligatory exchange. At early developmental stages, neuroepithelial cells constituting the ventricular zone expressed ASCT1 mRNA and protein ubiquitously. Thereafter, ASCT1 expression was gradually downregulated in neuronal populations during the late embryonic and neonatal periods, whereas its high expression was transmitted to radial glial cells and then to astrocytes. High levels of ASCT1 were also detected in the olfactory ensheathing glia. The preferential glial expression of ASCT1 was consistent with that of 3PGDH, and their extensive colocalization was demonstrated at the cellular level. Moreover, high cellular contents of L-Ser were revealed in these glial cells by using a specific antibody to L-Ser. These results strongly suggest that a large amount of L-Ser is synthesized and stored in these glial cells and is released through ASCT1 in exchange for other extracellular substrates. In addition, we observed prominent expression of ASCT1 in capillary endothelial cells of embryonic and neonatal brains. Therefore, ASCT1 appears to be regulated to meet metabolic demands by differentiating and mature neurons through the transport of glia- and blood-borne small neutral amino acids.

Key words: **amino acid transporter; ASCT1; L-Ser; astrocyte; capillary; brain; blood–brain barrier**

Introduction

L-Ser is synthesized in cells from the glycolytic intermediate 3-phosphoglycerate (Snell, 1984) and used for syntheses of various biomolecules, including other amino acids (Gly and L-Cys), proteins, membrane lipids (phosphatidyl-L-Ser and sphingolipids), and nucleotides. Emerging evidence indicates that L-Ser biosynthesis is essential for neuronal development and function. In *in vitro* studies, application of L-Ser or Gly greatly promotes survival and differentiation of cultured neurons (Savoca et al., 1995; Mitoma et al., 1998; Furuya et al., 2000). Enrichment of these amino acids in astrocyte-rich conditioned medium suggests the glia to be the source (Mitoma et al., 1998; Furuya et al., 2000; Verleysdonk and Hamprecht, 2000). In support of these findings, 3-phosphoglycerate dehydrogenase (3PGDH), the first step enzyme of the L-Ser biosynthetic pathway, is preferentially expressed in the radial glia–astrocyte lineage and olfactory ensheathing glia but not in neurons (Yamasaki et al., 2001). The physiological importance is further evidenced from inherited 3PGDH deficiency in humans; patients who have marked decreases in L-Ser and Gly in the plasma and CSF are afflicted with severe neurological disorders, such as congenital microcephaly, dysmyelination, seizures, and psychomotor retardation, but show beneficial effects through oral treatment of the deficient amino acids (Jaeken et al., 1996; de Koning et al., 1998, 2002; Klomp et al., 2000). However, how neurotrophic L-Ser is delivered to the neurons remains uncertain.

Cellular transport of amino acids is mediated by multiple transporter systems distinguished primarily by substrate specificity and ionic requirements (Christensen, 1990). In mammalian cells, small neutral amino acids, including L-Ser, are transported predominantly by Na^+-dependent transport system ASC (for Ala-, Ser-, and Cys-preferring) and system A (for Ala-preferring) and also by Na^+-independent transport system asc. Of these, we focused on the system, ASCT1, as a potential candidate for glia-derived L-Ser transporter for the following reasons. Although the system ASC is originally characterized to be Na^+-dependent, the system ASC does not use the Na^+ gradient for its driving force and instead mediates obligatory exchange of substrate amino acids (Arriza et al., 1993; Shafqat et al., 1993; Zerangue and Kavanaugh, 1996). This predicts that cells will release L-Ser in exchange for extracellular substrates if the system ASC is expressed in L-Ser-rich cells. Of two isoforms of system ASC transporters, the adult brain highly expresses ASCT1 (Arriza et al., 1993; Shafqat et al., 1993), whereas ASCT2 is low or undetectable (Kekuda et al., 1996; Utsunomiya-Tate et al., 1996).

Received Aug. 12, 2002; revised Oct. 28, 2002; accepted Oct. 30, 2002.

This work was supported by special coordination funds for promoting science and technology and a grant-in-aid for scientific research (B) and for scientific research on priority areas, all provided by the Ministry of Education, Culture, Sports, Science and Technology of the Japanese government. We thank Dr. Y. Hirabayashi [The Institute of Physical and Chemical Research (RIKEN) Brain Science Institute] for encouragement.

*K.S. and H.S. contributed equally to this work.

Correspondence should be addressed to Masahiko Watanabe, Department of Anatomy, Hokkaido University School of Medicine, Sapporo 060-8638, Japan. E-mail: watamasa@med.hokudai.ac.jp.

 0270-6474/03/230550-11$15.00/0

In the present study, we tested the hypothesis by using *in situ* hybridization and immunohistochemistry for ASCT1 in the developing and adult mouse brain. Here we show that ASCT1 is preferentially expressed in the radial glia–astrocyte lineage and olfactory ensheathing glia, all of which express 3PGDH selectively. Moreover, the specific antibody to L-Ser reveals its highly concentrated distribution in these glial cells, thus favoring our hypothesis. Furthermore, high and transient expression of ASCT1 is also found in embryonic and neonatal brain capillaries, which may underlie the known high activities of the transport system ASC at the blood–brain barrier in developing brains.

Materials and Methods

Animals and section preparation. Under deep pentobarbital anesthesia (100 mg/kg of body weight), brains of C57BL/6J mice were obtained at embryonic day 13 (E13), E15, E18, postnatal day 1 (P1), P7, P10, P14, P21, and adult (2–3 months). The day after overnight mating was counted as E0. For *in situ* hybridization, brains were freshly obtained and immediately frozen in powdered dry ice. Frozen sections (20 μm in thickness) were prepared on a cryostat (CM1900; Leica, Nussloch, Germany), mounted on silane-coated glass slides (Muto Pure Chemicals, Tokyo, Japan), and air-dried. For immunohistochemistry, embryonic brains were fixed by overnight immersion in Bouin's fixative, embedded in paraffin wax after dehydration using graded alcohols, and processed for the preparation of paraffin sections (5 μm) with a sliding microtome (SM2000R; Leica). Postnatal brains were perfused transcardially with 4% paraformaldehyde 0.1 M sodium phosphate buffer (PB), pH 7.4, and processed for paraffin or microslicer sections (50 μm, VT1000S; Leica). For immunoelectron microscopy, mice were perfused transcardially with 4% paraformaldehyde in 0.1 M PB containing 0.1–0.5% glutaraldehyde.

In immunohistochemistry for L-Ser, anesthetized mice were perfused transcardially with 37°C Kerebs–Henseleit buffer (in mM: 118 NaCl, 4.7 KCl, 2 $CaCl_2$, 1.2 $MgSO_2$, 1.2 KH_2PO_4, 25 $NaHCO_3$, and 1 glucose) for 45 sec and then with 50–100 ml of 37°C 0.5% paraformaldehyde, 5% glutaraldehyde, and 0.2% picric acid in 0.1 M PB. Brains were postfixed in the same fixative for 2 hr at room temperature.

In situ *hybridization.* Two antisense oligonucleotides were synthesized as probes for mouse ASCT1 mRNA. The sequence is 5′-CTCAGCGTGGTGAGGCCGAAGTAAGCAACAGCGATGCCACCCAGA-3′ and 5′-CTCGGGGCCTAGCTTCTTTAGAGCCACTCCTAACATCAGGGCAAA-3′, which correspond to nucleotide residues 447–491 and 796–840 of mouse ASCT1 cDNA (GenBank accession number U75215). They were processed for probe labeling with [^{33}P]dATP, prehybridization, hybridization, washing, and autoradiography to x-ray films and emulsion, as reported previously (Yamasaki et al., 2001). For nonisotopic detection, a digoxigenin-labeled antisense cRNA probe was used to detect mouse proteolipid protein (PLP) mRNA with a 2-hydroxy-3-naphtholic acid-2-phenylanilide phosphate fluorescent detection set (Roche Molecular Biochemicals, Mannheim, Germany), as reported previously (Yamasaki et al., 2001).

Antibody. Polyclonal antibodies to ASCT1, glucose transporter GluT1, and thymosin β4 were raised against amino acid residues 478–532 of mouse ASCT1, 460–492 of mouse GluT1 (GenBank accession number M23384), and 1–44 of mouse thymosin β4 (GenBank accession number BC018286). The polypeptides were expressed as glutathione *S*-transferase (GST) fusion proteins using pGEX4T-2 plasmid vector (Amersham Biosciences, Uppsala, Sweden). The fusion protein was purified with glutathione-Sepharose 4B (Amersham Biosciences), emulsified with Freund's complete adjuvant (Difco, Detroit, MI), and injected subcutaneously into female New Zealand White rabbits and Hartley guinea pigs at intervals of 2 weeks. Two weeks after the sixth injection, affinity-purified antibodies were prepared, first using protein G-Sepharose (Amersham Biosciences) and then using antigen peptides coupled to cyanogen bromide (CNBr)-activated Sepharose 4B (Amersham Biosciences). For the preparation of affinity media, polypeptides devoid of GST was obtained by elution of the cleaved polypeptide after in-column thrombin digestion of fusion proteins bound to glutathione-Sepharose.

We also produced an antibody specific to L-Ser in the rabbit, as reported previously (Aoki et al., 1987). Briefly, L-Ser (500 μmol; Wako

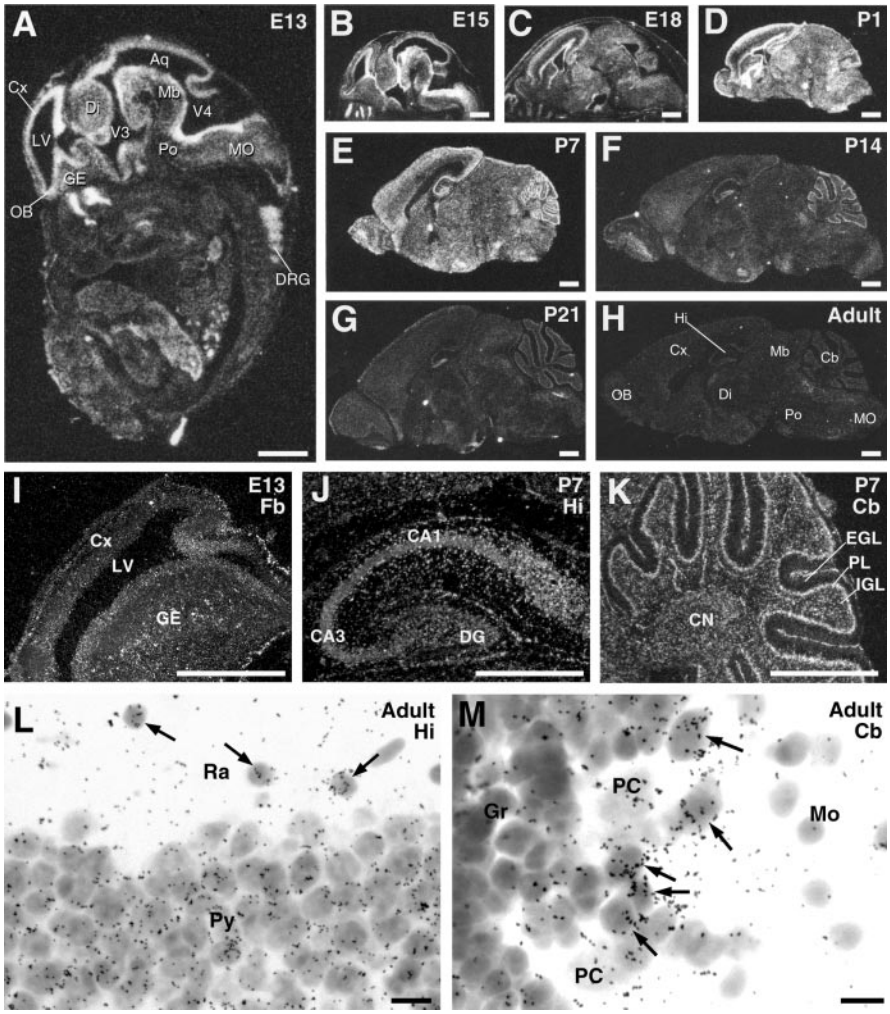

Figure 1. *In situ* hybridization for ASCT1 mRNA in the developing mouse brain. *A–H*, Negative images made from x-ray film autoradiograms of parasagittal brain sections at E13 (*A*), E15 (*B*), E18 (*C*), P1 (*D*), P7 (*E*), P14 (*F*), P21 (*G*), and adult (*H*). *I–K*, Enlarged dark-field images by emulsion microautoradiography in the forebrain (*Fb*) at E13 (*I*), hippocampus (*Hi*) at P7 (*J*), and cerebellum (*Cb*) at P7 (*K*). *L*, *M*, Bright-field images of the adult hippocampal CA1 (*L*) and cerebellar cortex (*M*), in which non-neuronal cells expressing ASCT1 mRNA are indicated by *arrows*. *Aq*, Cerebral aqueduct; *CA1, CA3*, CA1 and CA3 regions of the hippocampus; *CN*, deep cerebellar nuclei; *Cx*, cerebral cortex; *DG*, dentate gyrus; *Di*, diencephalon; *DRG*, dorsal root ganglion; *EGL*, external granular layer; *GE*, ganglionic eminence; *Gr*, granular layer; *IGL*, inner granular layer; *LV*, lateral ventricle; *Mb*, midbrain; *MO*, medulla oblongata; *Mo*, molecular layer; *OB*, olfactory bulb; *PC*, Purkinje cell; *PL*, Purkinje cell layer; *Po*, pons; *Py*, pyramidal cell layer; *Ra*, stratum radiatum; *V3, V4*, third and fourth ventricles. Scale bars: *A–K*, 1 mm; *L*, *M*, 10 μm.

Pure Chemical, Tokyo, Japan) and rabbit serum albumin (RSA, 50 mg; Sigma, St. Louis, MO) were dissolved in 10 ml of 0.2 M PB, and glutaraldehyde (500 μmol) was then added to initiate L-Ser–RSA conjugate formation. After incubation at 20°C for 20 hr, the reaction was terminated by adding 0.5 ml of $NaBH_4$ solution (4 mg/ml) and then dialyzed against 0.1 M PB for 48 hr at 4°C. Rabbits were immunized as above, and Igs were separated by protein G-Sepharose. The antibody specific to L-Ser was first purified using CNBr-activated Sepharose 4B coupled to the L-Ser–RSA conjugate, and then Igs cross-reacting to D-Ser and RSA were eliminated by passing the antibody through CNBr-activated Sepharose 4B coupled to the D-Ser–RSA conjugate.

Immunoblot. Adult mouse brains were homogenized in 4 volumes of buffer containing (in mM): 50 Tris-HCl, pH 7.4, 10 EDTA, 5 EGTA, 10 phenylmethylsulfonyl fluoride, and a protease inhibitor mixture for mammalian tissues (Sigma) and centrifuged at 1000 × *g* for 20 min to obtain postnuclear supernatants. The postnuclear supernatants were further centrifuged at 150,000 × *g* for 1 hr to obtain the membrane fraction. The protein concentration was determined by the method of Lowry et al. (1951). Fifty micrograms of protein samples were fractionated by 10% SDS-PAGE and electroblotted onto a nitrocellulose membrane (Schleicher & Schuell, Dassel, Germany). The blotted membrane was incubated with affinity-purified ASCT1 at 1 μg/ml in Tris-buffered saline (TBS; 50 mM Tris-HCl and 0.15 M NaCl, pH 7.4) containing 0.1% Tween 20 and 5% skim milk and visualized with an ECL chemiluminescence detection system (Amersham Biosciences, Bucks, UK).

Dot blot assay. To ascertain the sensitivity and specificity of the L-Ser antibody, various amino acids (Wako) were conjugated using glutaraldehyde to dialyzed cytosolic proteins of the mouse brain, followed by reduction with $NaBH_4$. Nitrocellulose membranes were spotted with 1 μl of dialyzed conjugates containing 10^{-8}, 10^{-9}, or 10^{-10} mol and probed with the L-Ser-specific antibody (1 μg/ml) in either the presence or absence of excess L-Ser conjugates. Procedures for immunoreaction and detection were done according to immunoblot.

Immunohistochemistry. For immunoperoxidase staining, parasagittal microslicer sections were incubated at room temperature with 10% normal sheep serum for 20 min, ASCT1 antibody (1 μg/ml) overnight, and peroxidase-linked secondary antibodies (1:200; Amersham Biosciences) for 2 hr. Immunoreaction was visualized with 3,3′-diaminobenzidine. For immunofluorescence, sections immunoreacted overnight with rabbit or guinea pig ASCT1 antibody (1–2 μg/ml) singly or in combination with rabbit GFAP antibody (1:10; Dako, Carpinteria, CA), rabbit 3PGDH antibody (1 μg/ml; Yamasaki et al., 2001), mouse MAP-2 antibody (1 μg/ml; Roche Molecular Biochemicals), rabbit GLAST antibody (1 μg/ml; Shibata et al., 1997), rabbit GluT1 antibody (1 μg/ml), or rabbit thymosin β4 (1 μg/ml) were incubated with a mixture of FITC- and Cy3-conjugated secondary antibodies for 2 hr (Jackson ImmunoResearch, West Grove, PA). Photographs were taken by a light microscope (AX-70; Olympus Optical, Tokyo, Japan) equipped with a digital camera (DP11; Olympus) or by a confocal laser scanning microscope (Fluoview; Olympus).

For L-Ser immunohistochemistry, microslicer sections were incubated at room temperature successively with 0.5% $NaBH_4$ in TBS for 20 min, TBS for 1 hr, 10% normal sheep serum for 1 hr, and rabbit L-Ser antibody (0.5 μg/ml) diluted with TBS containing 0.1% Triton X-100 overnight. They were further immunoreacted for immunoperoxidase with biotinylated goat anti-rabbit IgG for 3 hr and streptavidin–peroxidase complex for 30 min using a Histofine SAB-PO kit (Nichirei, Tokyo, Japan).

For immunoperoxidase electron microscopy, immunoreacted microslicer sections were further treated with 1% osmium tetroxide for 30–90 min and 2% uranyl acetate for 60 min, dehydrated using graded alcohols, and embedded in Epon 812. For silver-intensified immunogold, free-floating sections were first incubated with blocking solution consisting of TBS, 5% bovine serum albumin, and 0.02% saponin for 30 min. Sections were incubated overnight at 4°C with rabbit ASCT1 antibody (2 μg/ml) in the blocking solution and then with anti-rabbit IgG coupled to 1.4 nm gold (1:200; Nanoprobes, Stony Brook, NY). After postfixation with 1% glutaraldehyde in PBS for 10 min, silver enhancement of gold particles was done using an HQ silver kit (Nanoprobes) for 2–3 min.

Results

ASCT1 mRNA expression in developing and adult brains

By *in situ* hybridization with ^{33}P-labeled antisense probes, spatial and temporal patterns of ASCT1 mRNA expression were pursued in the mouse brain from E13 to the adult stage (Fig. 1). At E13, prominent expression was detected throughout the brain, with higher levels in the ventricular zone than in the mantle zone (Fig. 1*A*). Emulsion microautoradiography revealed the presence of intense signal clusters, which were dispersed against diffuse signals all over the ventricular and mantle zones (Fig. 1*I*). High expression levels in the brain were maintained from late embryonic stages until P7 (Fig. 1*B–E*). In the hippocampus at P7, prominent signals were detected in discrete cells dispersed all over the hippocampus, and moderate signals were observed in the pyramidal cell and granule cell layers (Fig. 1*J*). At this stage, high levels of ASCT1 mRNA also appeared in the Purkinje cell layer and the external and internal granular layers of the cerebellum (Fig. 1*K*).

Thereafter, expression levels were gradually decreased until the adult stage (Fig. 1*F–H*). At P21 and the adult stage, weak signals were distributed widely in the brain, showing no laminar distribution in the cerebral cortex (Fig. 1*G,H*). In the hippocam-

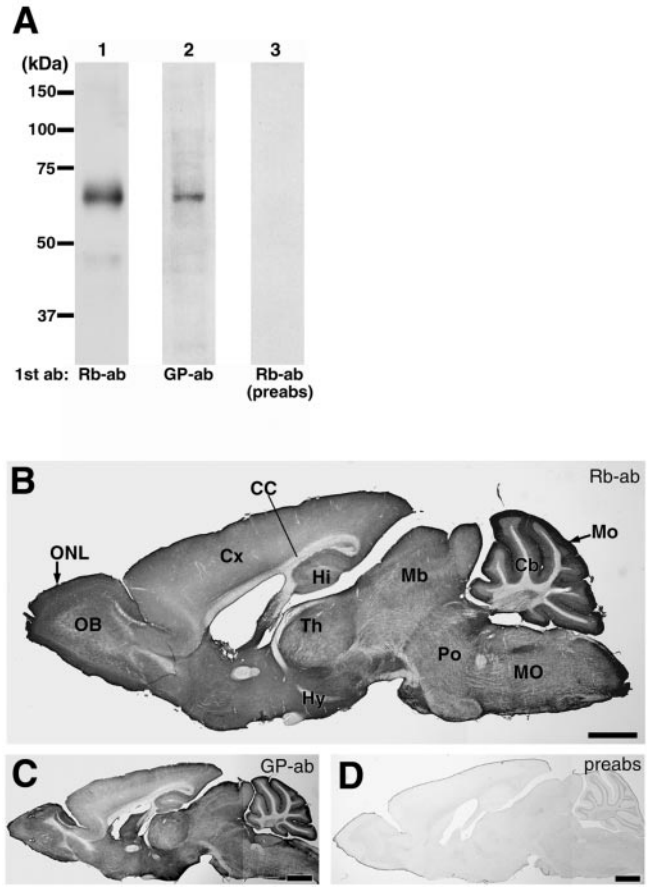

Figure 2. Specificity of ASCT1 antibody and immunohistochemistry. *A*, Immunoblot with ASCT1 antibodies. A protein band at 62~65 kDa is detected with rabbit (*Rb-ab*, *lane 1*) and guinea pig (*GP-ab*, *lane 2*) antibodies. This band is not visible with the use of the ASCT1 antibody preabsorbed with antigen (*preabs*, *lane 3*) or by omission of the primary antibody (data not shown). *B, C*, Immunoperoxidase with rabbit (*B*) and guinea pig (*C*) ASCT1 antibodies to parasagittal microslicer sections of the adult mouse brain. Note a similar distribution of immunoreactivities by the two antibodies, with particularly high immunoreactivities in the olfactory nerve layer (*ONL*) and cerebellar molecular layer (*Mo*). *D*, Control immunoperoxidase with preabsorbed rabbit ASCT1 antibody. *CC*, Corpus callosum; *Hy*, hypothalamus; *Th*, thalamus. See other abbreviations in the legend to Figure 1. Scale bars, 1 mm.

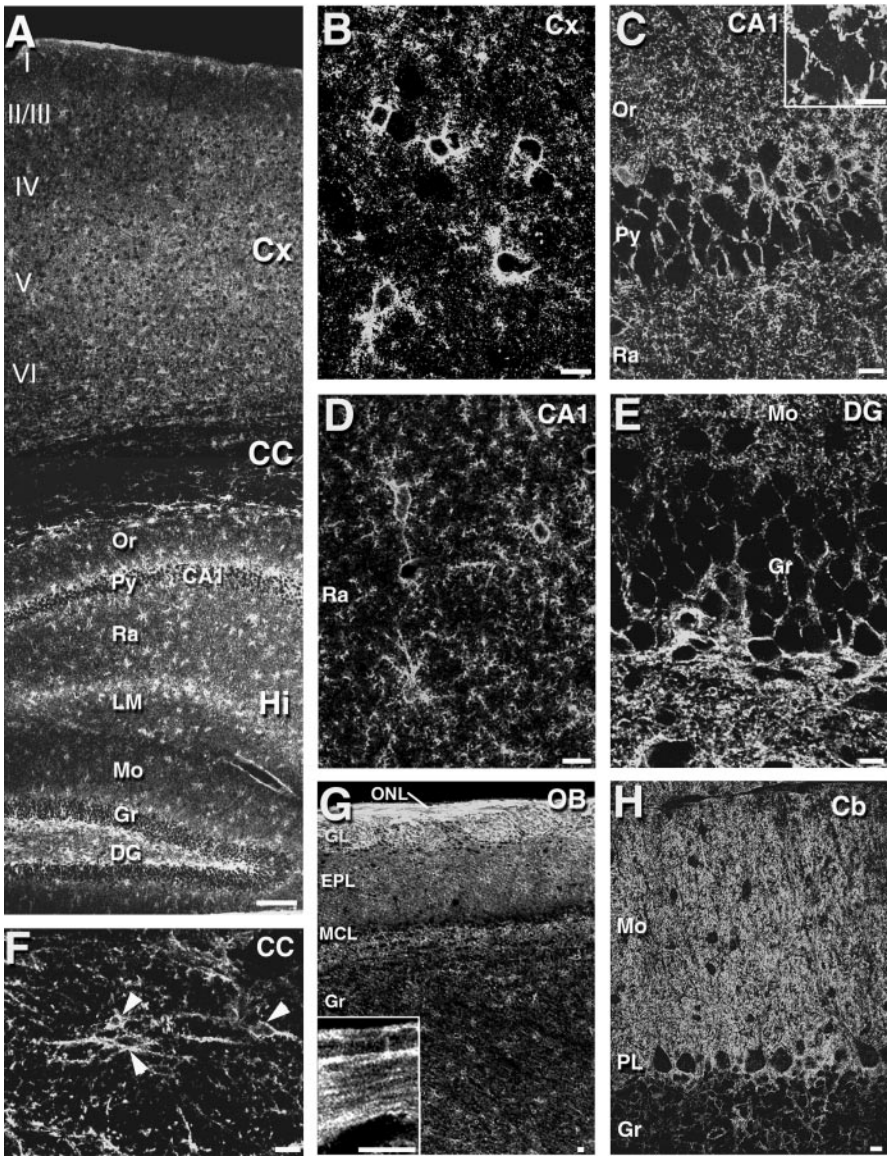

Figure 3. Immunofluorescence for ASCT1 in the adult mouse brain. *A*, An overview of ASCT1 immunostaining in the cerebral cortex (*Cx*), corpus callosum (*CC*), and hippocampus (*Hi*). *B–F*, Enlarged views of the cerebral cortex (*B*), hippocampal CA1 region (*C, D*), dentate gyrus (*E*), and corpus callosum (*F*). The *inset* in *C* shows the presence of low immunofluorescent puncta in pyramidal cell perikarya by raising the gain level of the confocal microscope. *Arrowheads* in *F* indicate ASCT1-positive cell bodies in the corpus callosum. *G*, Olfactory bulb. The *inset* in *G* is an enlarged image from the olfactory nerve layer (*ONL*). *H*, Cerebellar cortex. *EPL*, External plexiform layer; *GL*, glomerular layer; *LM*, stratum lacunosum-moleculare; *MCL*, mitral cell layer; *Or*, stratum oriens; *I–VI*, laminas I–VI of the cerebral cortex. See other abbreviations in the legend to Figure 1. Scale bars: *A*, 100 μm; *B–H*, 10 μm.

pus and cerebellar cortex, signals were detectable in pyramidal and Purkinje cells, but higher signals were often seen in adjacent non-neuronal cells having small dark nuclei (Fig. 1*L,M*).

Production of ASCT1 antibodies and specificity of immunohistochemistry

To determine cellular and subcellular expression, we produced affinity-purified polyclonal antibodies to ASCT1 in the rabbit and guinea pig. By immunoblot with the membrane fraction from adult mouse brain extracts, both antibodies strongly recognized a single protein band at 62~65 kDa (Fig. 2*A*), which is almost equivalent or slightly larger than the molecular mass calculated from 532 amino acid residues. By using ASCT1 antibodies preabsorbed with the antigen polypeptide (10 μg/ml), this band was abolished completely. By immunoperoxidase, rabbit and guinea pig antibodies similarly labeled various regions of the adult mouse brain, with the highest labeling in the cerebellar molecular layer and olfactory nerve layer (Fig. 2*B,C*). In the brain at E13, immunolabeling was higher in the ventricular zone than in the mantle zone (see Fig. 7*A*), consistent with the mRNA expression (Fig. 1*A*). When using preabsorbed antibodies, these immunohistochemical labelings were abolished (Fig. 2*D*; see Fig. 7*A*, *inset*), indicating the specificity of ASCT1 immunohistochemistry.

Cellular and subcellular localization in the adult brain

Using the ASCT1 antibodies, we investigated cellular expression and subcellular localization of ASCT1 in several regions of the adult brain.

Cerebral cortex

In the cerebral cortex, ASCT1 immunofluorescence was detected in small stellate cells, which were scattered evenly in the laminas I through VI (Fig. 3*A,B*). Among the immunostained cells, ASCT1 was also detected as tiny irregular puncta or ring-like structures in the neuropil (Fig. 3*B*). By double immunofluorescence for MAP-2 (*green*), a marker for neuronal perikarya and dendrites, ASCT1 (*red*) was very low or negative in MAP-2-positive neuronal elements (Fig. 4*A*). By double staining for GFAP, an astrocyte-specific intermediate filament, ASCT1 (*red*) was well overlapped with GFAP (*green*) in perikarya and perisomatic processes of astrocytes (Fig. 4*B*, *arrowhead*), although most of the ASCT1-labeled neuropil puncta were left unstained for GFAP. Immunoperoxidase electron microscopy revealed that immunolabeled puncta in the neuropil represented lamellate glial processes enwrapping synapses and dendrites (Fig. 5*A*). ASCT1 was also detected in GFAP-positive elements around capillaries (Fig. 4*B*), which were revealed by immunoelectron microscopy to be perivascular processes of astrocytes but not capillary endothelial cells (Fig. 5*B*). When examined for 3PGDH, a key enzyme of L-Ser biosynthesis, all of these ASCT1-immunopositive elements in the cortex (*red*) were costained for 3PGDH (Fig. 4*C*, *green*). Using thymosin β4 as a marker for microglia in the adult brain (Anadón et al., 2001), ASCT1 was not detected in thymosin-positive cells and processes, i.e., ramified or resting microglia (Fig. 4*D*).

Hippocampus

Similarly to the cortex, ASCT1 in the hippocampus was detected in small stellate cells and in punctate or ringed structures of the neuropil (Fig. 3*A,C–E*). Astrocytic expression of ASCT1 was confirmed by costaining with GFAP (data not shown) and by dense immunoelectron labeling in lamellate processes enwrapping neuronal somata, dendrites, and synapses (Fig. 5*C*). Coexpres-

sion of ASCT1 and 3PGDH was also confirmed by double immunofluorescence (data not shown). In contrast, ASCT1 was hardly detected in MAP-2-positive perikarya and dendrites of pyramidal cells (Fig. 4*E*). Because ASCT1 mRNA was observed in the pyramidal cell layer (Fig. 1*L*), neuronal expression of ASCT1 protein was carefully examined. By raising the gain level of the confocal scanning microscope, tiny punctate labeling for ASCT1 appeared in the perikaryon of pyramidal cells (Fig. 3*C*, *insets*), but they were much lower in intensity and smaller in size than the labeled structures of the astrocytes. By immunoelectron microscopy, weak ASCT1 labeling in neuronal perikarya was found around cisterns of the endoplasmic reticulum (ER) (Fig. 5*C*, *arrows*).

Corpus callosum

Compared with the gray matter, ASCT1 immunoreactivity was generally low in the white matter (Figs. 2*B,C*, 3*A*), but there were a few discrete cells expressing ASCT1 at high levels (Fig. 3*F*). In the corpus callosum, they possessed perisomatic processes, which were often oriented parallel to the nerve fibers (Fig. 3*F*) and were immunopositive for GFAP (Fig. 4*F*) and 3PGDH (Fig. 4*G*). Immunoelectron microscopy showed that ASCT1 was detected in irregular processes enwrapping synapses or associating myelinated fibers (Fig. 5*D*), indicating the presence of ASCT1 expression in callosal astrocytes. Because low to moderate expression of 3PGDH has been shown in oligodendrocytes (Yamasaki et al., 2001), we pursued the possibility of oligodendrocytic expression by double labeling for ASCT1 protein and PLP mRNA. Immunofluorescence for ASCT1 was not detected in PLP mRNA-positive callosal cells, indicating the lack of ASCT1 expression in callosal oligodendrocytes (Fig. 4*H,I*).

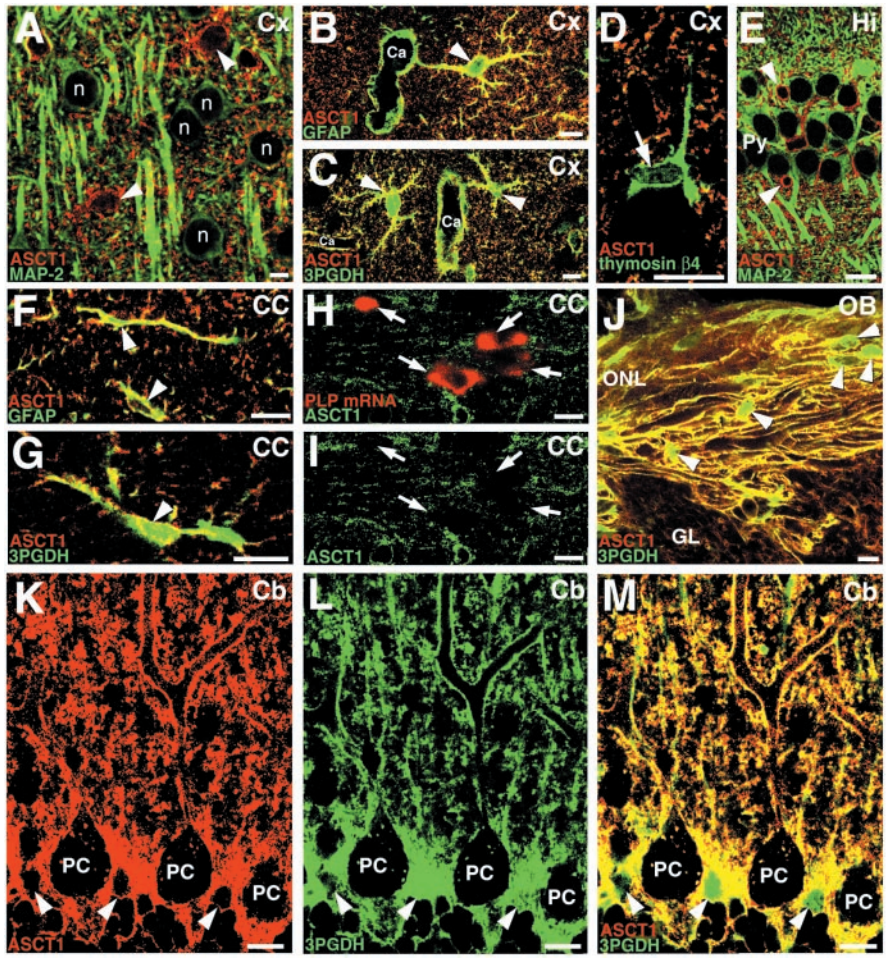

Figure 4. Double staining for ASCT1 and various cellular markers in the adult cerebral cortex (*A–D*), hippocampus (*E*), corpus callosum (*F–I*), olfactory bulb (*J*), and cerebellar cortex (*K–M*). In all *panels*, ASCT1-immunostained cells are indicated by *arrowheads*. *A*, Double immunofluorescence for ASCT1 (*red*) and MAP-2 (*green*) in the cortex. ASCT1 is not detected in MAP-2-positive neuronal cell bodies (*n*) or dendrites. *B*, ASCT1 (*red*) and GFAP (*green*) in the cortex. ASCT1 is detected in GFAP-positive astrocytes (*arrowhead*), whose processes often surround capillaries (*Ca*). *C*, Extensive costaining of ASCT1 (*red*) and 3PGDH (*green*) in the cortex. This image is quite similar to *B*. *D*, ASCT1 (*red*) and thymosin β4 (*green*). ASCT1 is not detected in thymosin-positive microglia (*arrow*). *E*, ASCT1 (*red*) and MAP-2 (*green*) in the hippocampus. *F*, Codistribution of ASCT1 (*red*) and GFAP (*green*) in callosal astrocytes. *G*, Codistribution of ASCT1 (*red*) and 3PGDH (*green*) in callosal astrocytes. *H, I*, Double staining for ASCT1 protein (*green*) and PLP mRNA (*red, arrows*) in the corpus callosum. ASCT1 expression is lacking in PLP mRNA-expressing oligodendrocytes. *J*, Extensive costaining of ASCT1 (*red*) and 3PGDH (*green*) in the olfactory nerve layer. The interior of olfactory ensheathing glia (*arrowheads*) is preferentially labeled for 3PGDH, reflecting its cytosolic distribution. *K–M*, Double immunofluorescence for ASCT1 (*red*) and 3PGDH (*green*) in the cerebellar cortex. Cell bodies (*arrowheads*) and radial fibers of Bergmann glia are costained for both. Note the low particulate immunofluorescence for ASCT1 in the interior of Purkinje cells (*PC*). Scale bars, 10 μm.

Olfactory bulb

In the olfactory nerve layer, ASCT1 was detected in fibrous structures parallel to the olfactory surface (Fig. 3*G*). ASCT1 was overlapped well with 3PGDH in the fibrous structures (Fig. 4*J*). By immunoelectron microscopy, ASCT1 was detected in lamellate processes enwrapping bundles of olfactory nerves (Fig. 5*E*), indicating its expression in the olfactory ensheathing glia. In deeper regions of the olfactory bulb, ASCT1-immunopositive cells were stellate in shape (Fig. 3*G*) and costained for GFAP and 3PGDH (data not shown), thus being common astrocytes.

Cerebellum

In the molecular layer of the cerebellum, ASCT1 was strongly detected in a fine reticular pattern (Fig. 3*H*). By immunofluorescence, intense ASCT1 immunofluorescence fringed cell bodies and stem dendrites of Purkinje cells and was also distributed irregularly in the neuropil (Fig. 4*K*). In contrast, the interior of Purkinje cell soma and dendrites was generally low, except for the intracellular tiny puncta (Fig. 4*K*). When merged with 3PGDH (Fig. 4*L*), which is known to be abundant in and selective to Bergmann glial cells in the molecular layer (Furuya et al., 2000; Yamasaki et al., 2001), ASCT1 was almost completely overlapped with 3PGDH (Fig. 4*M*). By immunoperoxidase electron microscopy, intense immunolabeling was detected in lamellate glial processes surrounding Purkinje cell dendrites, synapses, and capillary endothelial cells (Fig. 6*A–D*). ASCT1 was almost negative in presynaptic terminals, postsynaptic spines, and capillary endothelial cells (Fig. 6*C,D*). Silver-enhanced immunogold visualized that metal particles representing ASCT1 were preferentially associated with the cytoplasmic side of the cell membrane of the Bergmann glia (Fig. 6*E,F*). In perivascular sheets of Bergmann glia, immunogold particles were observed in the cell membranes

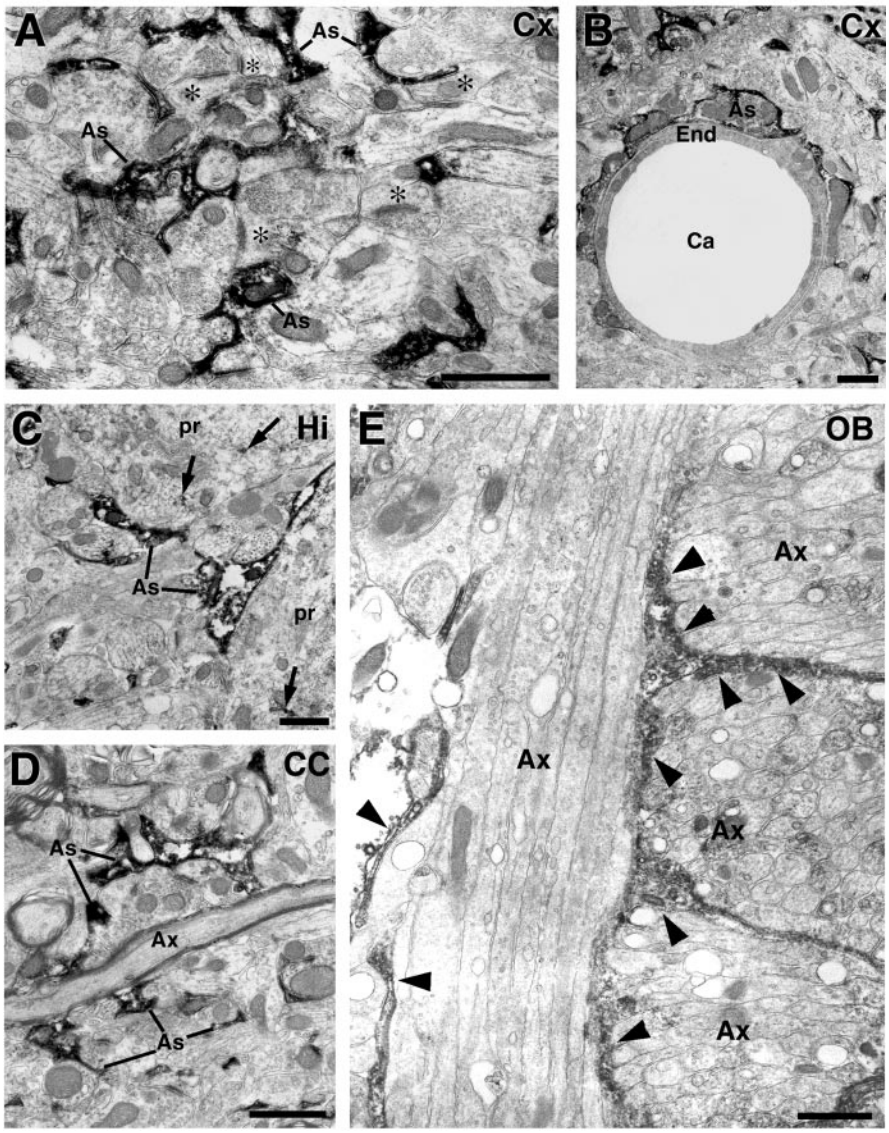

Figure 5. Immunoperoxidase electron microscopy for ASCT1 in the adult telencephalon. *A*, *B*, Cerebral cortex. Note dense ASCT1 labeling in astrocytic processes (*As*) surrounding synapses (*asterisks*) and endothelial cells (*End*) of capillaries (*Ca*). *C*, Hippocampal CA1 region. In addition to intense labeling in astrocytic processes, low immunoreactivity is focally detected around the ER (*arrows*) within pyramidal cell perikarya (*pr*). *D*, Corpus callosum. Intense labeling is detected in astrocytic processes around callosal synapses and axons, whereas axons (*Ax*) and the myelin sheath are immunonegative to ASCT1. *E*, Olfactory bulb. *Arrowheads* indicate ASCT1-positive processes of the olfactory ensheathing glia, which surround bundles of unmyelinated olfactory nerve axons. Scale bars, 1 μm.

apposing both capillary and brain parenchyma (Fig. 6*G*). Inside Purkinje cell dendrites, cisterns of the ER were locally labeled by immunoperoxidase (Fig. 6*A*,*B*, *arrows*) and immunogold (Fig. 6*E*), whereas the cell membrane of Purkinje cell dendrites was not labeled for ASCT1.

Cellular expression during brain development

Cellular expression of ASCT1 was further examined in the developing brain, mainly using the cerebral cortex (Figs. 7, 8*A–C*). At E13, when the cerebral cortex was exclusively composed of neuroepithelial cells with a thin overlying preplate, ASCT1 was detected intensely in various cellular elements within the wall or on the surface of the brain (Fig. 7*B*). First, ASCT1 was overlapped with 3PGDH in neuroepithelial cells constituting the ventricular zone, radial fibers running through the preplate, and the glia limitans covering the brain surface (Fig. 7*C*). Second, ASCT1 was detected in perikarya of MAP-2-positive preplate neurons (Fig. 7*D*, *arrowheads*). Third, intense labeling for ASCT1 often yielded ring-like or tubular patterns, which were immunonegative to 3PGDH (Fig. 7*B,C*, *arrows*). By use of an antibody specific to glucose transporter GluT1, ASCT1 was overlapped with GluT1 in ringed structures in the brain wall and surface, indicating its expression in capillaries (Fig. 7*E*). These light microscopic observations were confirmed by immunoelectron microscopy in the cerebral cortex at E15 (Fig. 8*A–C*). Immunoperoxidase products for ASCT1 were detected in the thin perikarya of neuroepithelial cells (Fig. 8*A*) and capillary endothelial cells (Fig. 8*B*). By immunogold, the luminal and abluminal cell membranes of capillary endothelial cells were labeled (Fig. 8*C*).

At E18, when the cortex was remarkably thickened, and numerous oval neurons formed a thick cortical plate, intense ASCT1 immunoreactivities were observed in capillaries, neuroepithelial cells in the ventricular zone, and radial fibers running through the cortical plate and marginal zone (Fig. 7*F*). Of these, neuroepithelial cells and radial fibers were costained for 3PGDH, whereas capillaries were negative to 3PGDH and instead surrounded by thin sheets expressing both ASCT1 and 3PGDH (Fig. 7*G,H,J*). At this stage, a few slender cells, which projected radial fibers and possessed 3PGDH, appeared in the cortical plate (Fig. 7*G,H*, *arrowheads*). Because these slender cells and radial fibers expressed Glu transporter GLAST (Fig. 7*I*), a marker for the radial glia/astrocyte lineage, they were judged to be glial cells, presumably migrating radial glia or astrocytes. Cortical neurons were stained for ASCT1, but the intensity was lower than the adjacent radial fibers and glial cells (Fig. 7*G,H*). Neuronal ASCT1 was further downregulated after birth; at P7, it was detected very weakly in MAP-2-positive perikarya (Fig. 7*K*), in sharp contrast to the strong immunolabeling in GLAST-positive astrocytes (Fig. 7*L*).

We pursued the developmental loss of ASCT1 expression in capillaries. In the cerebral cortex at P7, ASCT1 was coexpressed with GluT1 in many capillaries (Fig. 7*M*). At P10, two types of capillaries were distinguished, i.e., those coexpressing ASCT1 and GluT1 (Fig. 7*N*) and those expressing GluT1 but not ASCT1 (Fig. 7*O*). At P14, the second type of capillaries became the majority in the cerebral cortex (82%) (Fig. 7*P*), and was covered with perivascular sheets costained for ASCT1 and 3PGDH (Fig. 7*P,Q*).

A similar developmental transition of ASCT1 expression in capillaries was shown in the cerebellar cortex at P10 (Fig. 8*D–F*). Capillary endothelial cells were either labeled (Fig. 8*D*) or unlabeled (Fig. 8*F*) for ASCT1. In labeled capillaries, immunogold was depos-

ited in both the luminal and abluminal cell membranes (Fig. 8*E*). On the other hand, unlabeled capillaries were surrounded by ASCT1-immunoreactive perivascular sheets of Bergmann glia (Fig. 8*F*). Thereafter, capillary endothelial cells lacking ASCT1 became common in the cerebellum as well. Therefore, ASCT1 expression is lost from capillaries during the second postnatal week.

L-Ser is richly contained in ASCT1-expressing glial cells but not in capillary endothelial cells

Finally, an L-Ser-specific antibody was produced to examine L-Ser contents in ASCT1-expressing cells (Fig. 9). As expected, the L-Ser antibody selectively recognized L-Ser conjugated to brain cytosolic proteins but not unconjugated cytosolic proteins or other amino acid conjugates (Fig. 9*A*). The L-Ser antibody widely stained the adult mouse brain (Fig. 9*B*). The use of the L-Ser antibody preabsorbed with an excess amount of the L-Ser conjugate completely abolished the immunoreaction in dot blot assay (Fig. 9*A*) and immunohistochemistry (Fig. 9*C*). As reported previously (Yasuda et al., 2001), L-Ser immunoreactivities were detected in glial and neuronal populations, showing regional differences. In the olfactory nerve layer, strong L-Ser immunoreactivities were detected in perikarya of the olfactory ensheathing glia, and their processes were enwrapping olfactory nerves (Fig. 9*G*). In the hippocampus, L-Ser immunoreactivities were detected in both neuronal (pyramidal cells and apical dendrites) and glial elements (Fig. 9*D*). Intense immunolabeling in glial cells was also shown in the corpus callosum (Fig. 9*E*). In the cerebellar cortex, cell bodies and radial fibers of the Bergmann glia were quite intense for L-Ser, whereas Purkinje cells were very low (Fig. 9*F*,*H*). Despite the regional differences in neuronal staining, high cellular contents of L-Ser were thus consistent in particular glial cells that coexpress ASCT1 and 3PGDH.

L-Ser was further examined in capillary endothelial cells at P7, when ASCT1 was expressed at high levels. However, L-Ser immunoreactivities were low or undetectable in endothelial cells and, instead, detected at high levels in astrocytic processes associated with capillaries (Fig. 9*I*).

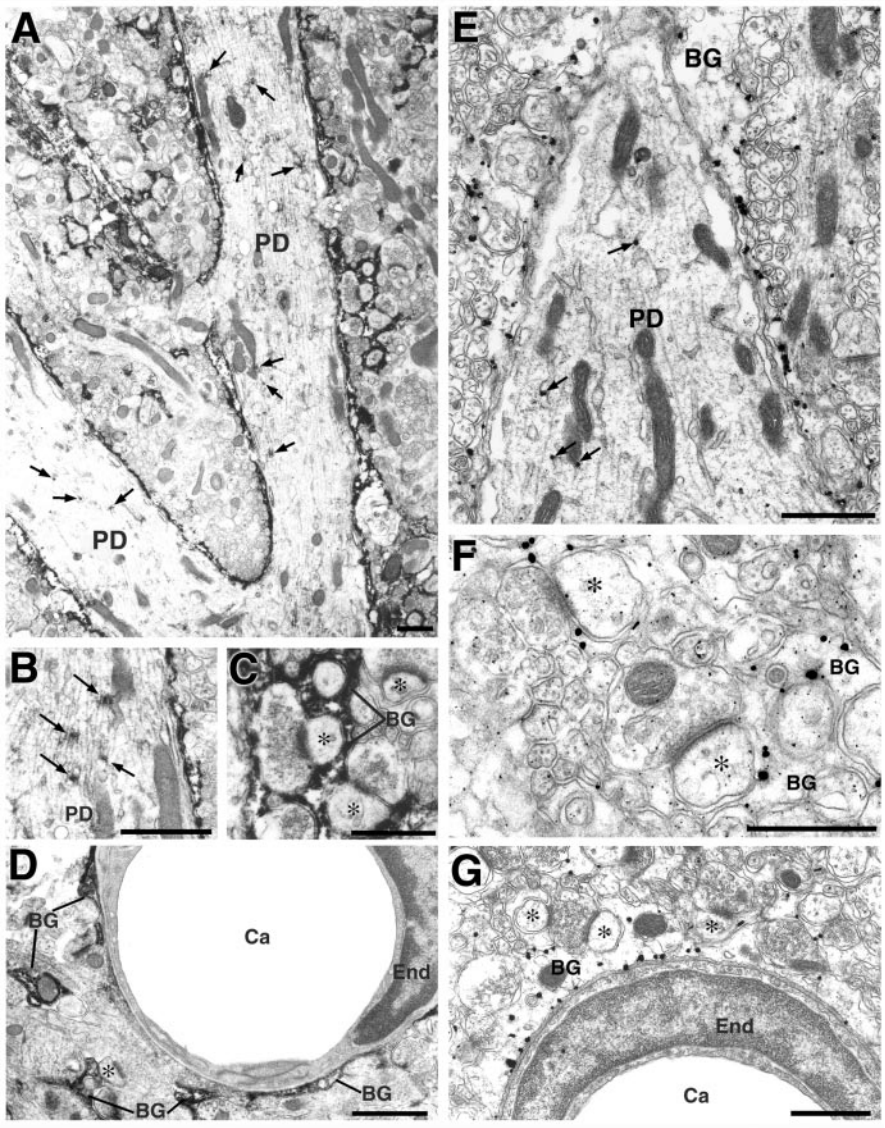

Figure 6. Immunoperoxidase (*A–D*) and silver-enhanced immunogold (*E–G*) electron microscopy for ASCT1 in the adult cerebellum. Intense immunoreaction is detected in processes of Bergmann glia (*BG*), which surround Purkinje cell dendrites (*PD*), synapses (*asterisks*), and endothelial cells (*End*) of capillaries (*Ca*). Low focal immunostaining is also detected in Purkinje cell dendrites around the ER (*arrows*). Scale bars, 1 μm.

Discussion

In the present study, we examined the expression of the neutral amino acid transporter ASCT1 in developing and adult mouse brains by *in situ* hybridization and immunohistochemistry. We have disclosed the distinct cellular expression and temporal regulation. A preceding paper reported a different immunohistochemical distribution of ASCT1 in the developing rat brain using a commercial polyclonal antibody against human ASCT1 (Weiss et al., 2001); predominant neuronal immunostaining and the lack of capillary staining are inconsistent with our results. Our antibody was raised against mouse ASCT1, and its specificity has been characterized by biochemical and histochemical examinations with mouse brain tissues (Fig. 2) as well as by consistent expression patterns by *in situ* hybridization (Fig. 1). Furthermore, we also obtained similar cellular expression in the rat brain (data not shown).

ASCT1 is the most likely transporter mediating the release of glia-borne L-Ser to neighboring cells

We have proposed previously that L-Ser serves as a major astrocyte-derived trophic factor for developing neurons, based on the following facts: (1) L-Ser, Gly, and Ala are actively released into glia-rich culture medium; (2) exogenous L-Ser and Gly but not Ala display striking trophic effects on the survival and differentiation of cultured neurons; (3) L-Ser and Gly are interconvertible by serine hydroxymethyltransferase; and (4) the L-Ser biosynthetic enzyme 3PGDH is selectively expressed in particular glial populations after the stage of

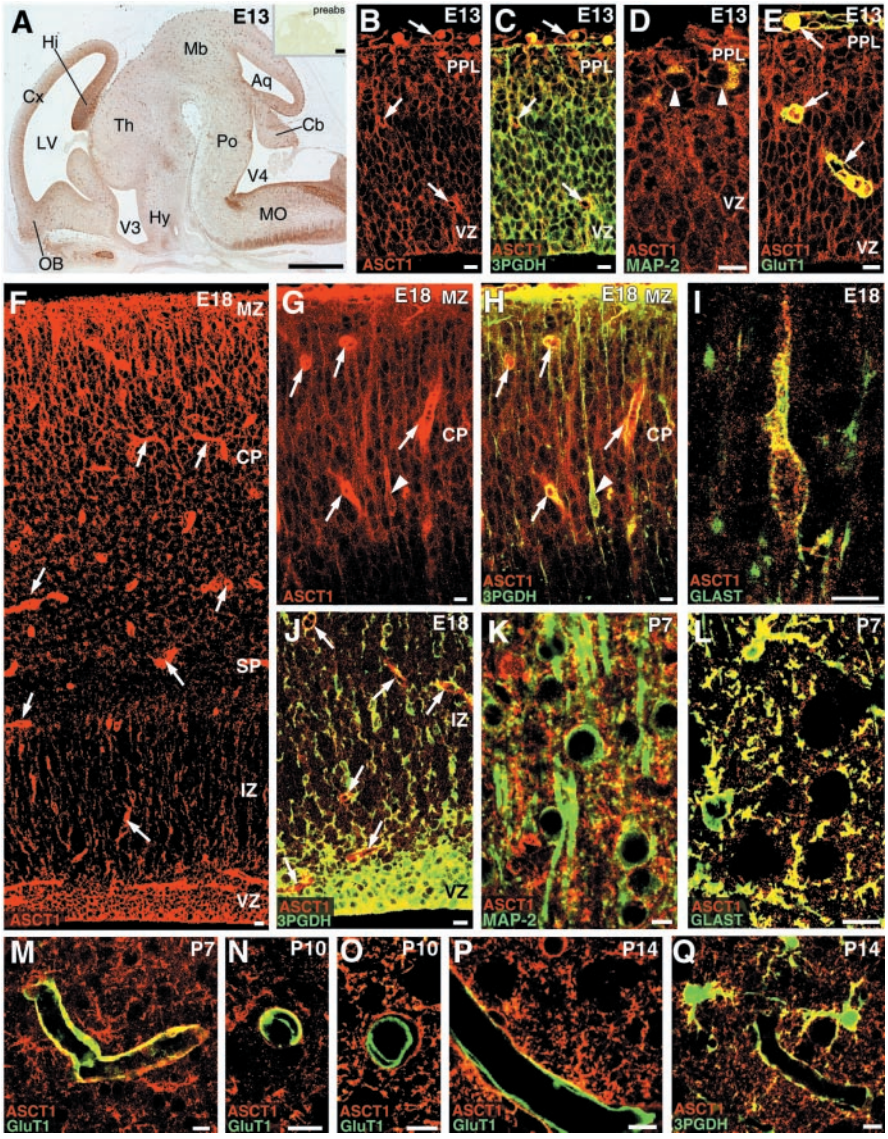

Figure 7. Cellular expression of ASCT1 in the developing cerebral cortex at E13 (*A–E*), E18 (*F–J*), P7 (*K–M*), P10 (*N, O*), and P14 (*P, Q*). *A*, Overview of ASCT1 immunostaining in the parasagittal brain section at E13. Intense ASCT1 staining is observed in the ventricular zone (*VZ*) and tubular profiles all over the brain wall. The *inset* shows negative immunostaining with the use of preabsorbed antibody (*preabs*). *B, C*, Double immunofluorescence for ASCT1 (*red*) and 3PGDH (*green*). *B*, Single fluorescent image for ASCT1; *C*, merged view with 3PGDH. *Arrows* indicate tubular structures immunopositive for ASCT1 but not for 3PGDH. *D*, ASCT1 (*red*) and MAP-2 (*green*). MAP-2-positive neurons (*arrowheads*) in the preplate (*PPL*) are immunoreactive to ASCT1. *E*, ASCT1 (*red*) and GluT1 (*green*). Capillaries (*arrows*) are immunoreactive to both ASCT1 and GluT1. *F*, Single immunofluorescence for ASCT1 at E18. *G, H*, Double immunofluorescence for ASCT1 (*red*) and 3PGDH (*green*) in the superficial cortical region at E18. *G*, Single image for ASCT1; *H*, merged image with 3PGDH. Note intense fluorescence in radial fibers running in the cortical plate (*CP*) and marginal zone (*MZ*) as well as in capillaries (*arrows*). Also note a slender cell with radial fibers (*arrowhead*), which is immunoreactive to both ASCT1 and 3PGDH. *I*, ASCT1 (*red*) and GLAST (*green*). Such slender cells with radial fibers are immunoreactive to GLAST, indicating migrating radial glia cells or astrocytes. *J*, ASCT1 (*red*) and 3PGDH (*green*) in the deep region of the cortex. Note intense double fluorescence in neuroepithelial cells of the ventricular zone (*VZ*) and in dispersed cells of the intermediate zone (*IZ*). *K*, Nonoverlapping pattern for ASCT1 (*red*) and MAP-2 (*green*) at P7. *L*, Extensive costaining for ASCT1 (*red*) and GLAST (*green*) at P7. *M–P*, Double immunofluorescence for ASCT1 (*red*) and GluT1 (*green*) showing the loss of capillary expression of ASCT1 during the second postnatal week. At P7, most capillaries are immunoreactive to both ASCT1 and GluT1 (*M*). At P10, two types of capillaries are observed, one retaining ASCT1 expression (*N*) and the other lacking ASCT1 (*O*). At P14, many capillaries are negative to ASCT1 (*P*). *Q*, ASCT1 (*red*) and 3PGDH (*green*) at P14. ASCT1 and 3PGDH are well overlapped in astrocytes and also in their processes surrounding capillaries. *Hy*, Hypothalamus; *SP*, subplate; *Th*, thalamus. See other abbreviations in the legend to Figure 1. Scale bars: *A*, 0.5 mm; *B–Q*, 20 μm.

neuroepithelium during brain development (Mitoma et al., 1998; Furuya et al., 2000; Yamasaki et al., 2001). To seek the molecular candidates for the release of glia-borne L-Ser, we started the present molecular and anatomical investigation on ASCT1. Here we demonstrate that ASCT1 expression is ubiquitous in neuroepithelial cells in the very early stage of brain development, and that its high expression is transmitted preferentially to particular glial populations (i.e., radial glia and astrocytes). In astrocytes of the adult brain, ASCT1 is localized on the cell membrane. In addition to these brain-derived glial cells, ASCT1 is highly expressed in the olfactory ensheathing glia, which originates peripherally from the olfactory placode, directly enwraps olfactory nerves that continue to regenerate throughout an animal's life, and exhibits growth-promoting activities for growing and regenerating axons (Marin-Padilla and Amieva, 1989; Doucette, 1991; Ramón-Cueto, 2000). Importantly, all of these glial cells express 3PGDH abundantly and selectively (Yamasaki et al., 2001; double immunofluorescence in this study). ASCT1 is a member of the amino acid transport system ASC, being characterized by a preference for small neutral amino acids (Christensen et al., 1967). ASCT1, although requiring extracellular Na^+ in its transport, mainly mediates homoexchange and heteroexchange of the substrate amino acids, such as Ala, Ser, Cys, and Thr, rather than their net uptake (Zerangue and Kavanaugh, 1996). In the adult brain, we have further shown intense L-Ser immunoreactivities in astrocytes and olfactory ensheathing glia that coexpress ASCT1 and 3PGDH. Taken together, it is very likely that a large amount of L-Ser is synthesized and stored in these glial cells and released to the extracellular space through ASCT1 (Fig. 10*B*), probably in exchange for other substrate amino acids. On the other hand, oligodendrocytes possess low levels of 3PGDH in perikarya (Yamasaki et al., 2001) but lack ASCT1 expression. This implies that a small amount of L-Ser is synthesized in oligodendrocytes for their own use, unless other relevant transporters are expressed.

There are several other candidates for L-Ser transport. Expression of ASCT2 in astrocytes has been reported by PCR (Bröer et al., 1999), but the level appears very low in the brain (Kekuda et al., 1996; Utsunomiya-Tate et al., 1996). The system asc is characterized by Na^+-independent transport of small neutral amino acids, and two members, Asc-1 and Asc-2, have been identified. Asc-1 is highly expressed in the brain, but the type of cells expressing it has not yet been clarified (Fukasawa et al., 2000; Chairoungdua et al., 2001). Despite the fragmental information on other relevant transporters, coincidental distribution of 3PGDH, ASCT1, and high L-Ser contents in particular glial cells strongly suggests that ASCT1 is the major transporter responsible for the release of glia-borne L-Ser to neighboring cells.

ASCT1 is unlikely to mediate neuronal uptake of small neutral amino acids

ASCT1 immunoreactivities are detected in immature neurons in the embryonic cortical plate but are gradually downregulated as they differentiate. ASCT1 mRNA is still detectable in adult neurons, but the immunoreactivities are not detected in their cell membrane. Thus, ASCT1 is unlikely to mediate the transport of small neutral amino acids across the neuronal cell membrane.

It has been reported that neurons express system A transporter 1 (SAT1) and SAT2 (Reimer et al., 2000; Varoqui et al., 2000; Yao et al., 2000; Armano et al., 2002; Chaudhry et al., 2002). They are Na^+-dependent, unidirectional, and highly concentrative transporters preferring small neutral amino acids, such as Ala, Ser, and Gln. Glu is the major excitatory neurotransmitter in the CNS and plays multifarious roles in activity-dependent modification of synaptic circuitry and in the pathogenesis of excitotoxic neuronal death (Nakanishi et al., 1998). Synaptically released Glu is rapidly taken into astrocytes by high-affinity Glu transporters GLT1 and GLAST, and Gln synthetase converts Glu into Gln in astrocytes (Fig. 10*B*). System N transporter SN1, which is expressed selectively in astrocytes, is then implicated in both Gln influx and efflux depending on the Na^+ and H^+ gradients (Chaudhry et al., 1999; Gu et al., 2000; Boulland et al., 2002). In addition, astrocytic ASCT2, which transports Gln with high affinity, is also suggested to mediate Gln efflux (Bröer et al., 1999). On the basis of the expression and functional properties, the emerging picture has been proposed that these transporters cooperatively constitute the Glu–Gln cycle to maintain the homeostasis of the glutamatergic signaling system at central synapses (Magistretti et al., 1999; Bröer and Brookes, 2001). Similarly, it is conceivable that ASCT1 and system A transporters cooperate to mediate L-Ser supply from glia to neurons (Fig. 10*B*) to promote neuronal survival and differentiation (Furuya et al., 2000).

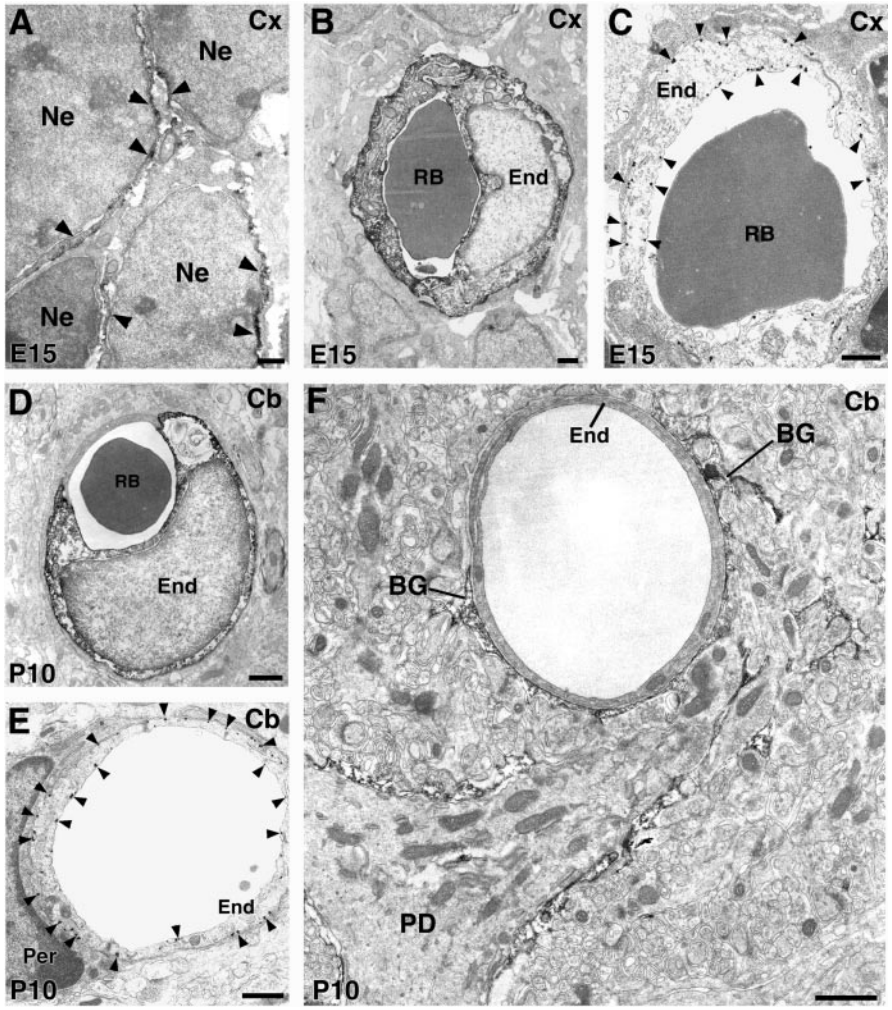

Figure 8. Immunoelectron microscopy for ASCT1 in the developing cerebral cortex at E15 (*A–C*) and cerebellar cortex at P10 (*D–F*). *A*, ASCT1 labeling is detected in the surface (*arrowheads*) of neuroepithelial cells (*Ne*). *B*, Immunoperoxidase labeling for endothelial cells (*End*) of cortical capillaries at E15. *C*, Immunogold labels the luminal and abluminal cell membranes of endothelial cells (*arrowheads*). *D*, Immunoperoxidase labeling of endothelial cells of cerebellar capillaries at P10. *E*, Immunogold labels the luminal and abluminal cell membranes of endothelial cells (*arrowheads*). *F*, Some capillaries at P10 lose ASCT1 expression and are surrounded by Bergmann glia processes (*BG*) with intense ASCT1 labeling. *Per*, Pericyte; *RB*, red blood cell. Scale bars, 1 μm.

It was unexpected for us to find that ASCT1 is present, although at low levels, around cisterns of the ER in neurons. ASCT1 on the ER can be interpreted as intracellular trafficking on the way to the cell membrane of neurons. In this case, we need to postulate that the local concentration of ASCT1 would decrease below the threshold of immunohistochemical detection after incorporation into the cell membrane. Alternatively, neuronal ASCT1 might actually function on the ER membrane. In that case, such ER might serve as an intracellular store or buffer by exchange of substrate amino acids between the cytoplasm and the ER lumen.

Transient ASCT1 expression in capillaries underlies high ASC transport activities across the blood–brain barrier in the developing brain

During the embryonic and neonatal periods, prominent expressions of ASCT1 mRNA and immunoreactivity are detected in brain capillaries. In these periods, both luminal and abluminal cell membranes of capillary endothelial cells are labeled. However, capillary expression of ASCT1 is substantially decreased to low or undetectable levels during the second postnatal week. The transient ASCT1 expression and the lack of 3PGDH expression in developing capillaries as well as low L-Ser contents may stand for high transport activities of small neutral amino acids across the blood–brain barrier (Fig. 10*A*). Indeed, it is known that transport activities of the system ASC are high in neonates but substantially decrease to low or undetected levels in adults (Wade and Brady, 1981; Lefauconnier and Trouve, 1983; Sánchez del Pino et al., 1992, 1995). Because L-Ser serves as a building block for proteins and indispensable precursors for membrane lipids (phosphatidyl-L-Ser and sphingolipids) and nucleotides (Snell, 1984; Stryer, 1995), a higher demand for the amino acid should be associated with developing brains, where neural cells proliferate and differentiate by extending neurites and glial processes. The transient ASCT1 expression in brain capillaries may contribute to the active transport system ASC across the blood–brain barrier in fetal and neonatal brains. It thus appears that blood-borne L-Ser, together with glia-borne L-Ser, plays an important

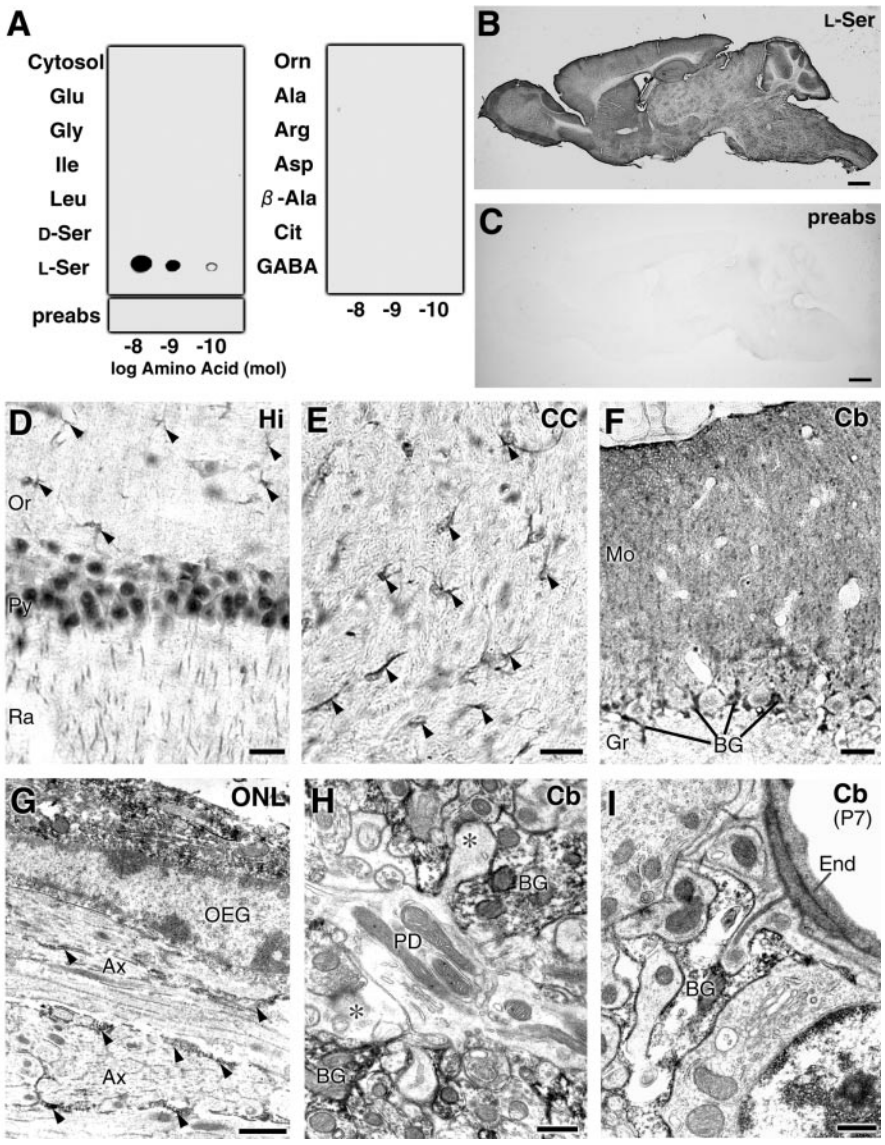

Figure 9. Specificity of L-Ser antibody and enriched glial distribution of L-Ser immunoreactivities in the adult mouse brain. *A*, Dot blot assay of the L-Ser antibody. Glutaraldehyde-mediated conjugates with brain cytosolic proteins (*Cytosol*) of various amino acids: L-*Glu*, *Gly*, *Ile*, *Leu*, D-*Ser*, L-*Ser*, L-*Orn*, L-*Ala*, L-*Arg*, L-*Asp*, β-*Ala*, L-*Cit*, and *GABA*. The L-Ser antibody preabsorbed with L-Ser– cytosolic protein conjugates (*preabs*) yields no immunoreacted spots. *B*, *C*, Light microscopic immunoperoxidase for L-Ser in the adult mouse brain in the absence (*B*) or presence (*C*) of L-Ser– cytosolic protein conjugates for preabsorption. *D–F*, Immunoperoxidase for L-Ser in the hippocampus (*D*), corpus callosum (*E*), and cerebellar cortex (*F*) of the adult mouse brain. *Arrowheads* in *D* and *E* indicate glial cells stained for of L-Ser. Note intense immunostaining in cell bodies and radial fibers of Bergmann glia (*BG*). *G–I*, Electron microscopic immunoperoxidase for L-Ser in the adult olfactory nerve layer (*G*) and in the cerebellar molecular layer at adult (*H*) and P7 (*I*). Note that intense L-Ser immunoreactivities are observed in perikarya and processes of the olfactory ensheathing glia (*OEG*; *G*) and Bergmann glia (*BG*; *H*, *I*). At P7, when capillaries express ASCT1, immunolabeling for capillary endothelial cells (*End*) is low or negative to L-Ser, representing low cellular contents of this amino acid. Scale bars: *B*, *C*, 1 mm; *D–F*, 20 μm; *G–I*, 1 μm.

role for satisfying the elevated demand for neutral amino acids in developing brains (Fig. 10*A*). On the other hand, the downregulation of ASCT1 expression and system ASC function in the early postnatal period may reflect either lowered demand for small neutral amino acids from the circulation or increased synthesis of these amino acids in local glial cells. This temporal regulation of ASCT1 is in contrast with that of the system L transporter, which prefers large neutral amino acids. The transport system L is richly provided both functionally and molecularly to the blood–brain barrier from the developing through the adult stages (Lefauconnier and Trouve, 1983; Boado et al., 1999; Matsuo et al., 2000).

Through the present investigation, we conclude that ASCT1 is the most likely candidate for the release of glia-borne L-Ser throughout brain development and also for active transport of small neutral amino acids at the blood–brain barrier during the fetal and neonatal periods.

References

Anadón R, Rodriguez Moldes I, Carpintero P, Evangelatos G, Livianou E, Leondiadis L, Quintela I, Cervino MC, Gomez-Marquez J (2001) Differential expression of thymosins β4 and β10 during rat cerebellum postnatal development. Brain Res 894:255–265.

Aoki E, Semba R, Kato K, Kashiwamata S (1987) Purification of specific antibody against aspartate and immunocytochemical localization of aspartergic neurons in the rat brain. Neuroscience 21:755–765.

Armano S, Coco S, Bacci A, Pravettoni E, Schenk U, Verderio C, Varoqui H, Erickson JD, Matteoli M (2002) Localization and functional relevance of system A neutral amino acid transporters in cultured hippocampal neurons. J Biol Chem 277:10467–10473.

Arriza JL, Kavanaugh MP, Fairman WA, Wu YN, Murdoch GH, North RA, Amara SG (1993) Cloning and expression of a human neutral amino acid transporter with structural similarity to the glutamate transporter gene family. J Biol Chem 268:15329–15332.

Boado RJ, Li JY, Nagaya M, Zhang C, Pardridge WM (1999) Selective expression of the large neutral amino acid transporter at the blood-brain barrier. Proc Natl Acad Sci USA 96:12079–12084.

Boulland JL, Osen KK, Levy LM, Danbolt NC, Edwards RH, Storm-Mathisen J, Chaudhry FA (2002) Cell-specific expression of the glutamine transporter SN1 suggests differences in dependence on the glutamine cycle. Eur J Neurosci 15:1615–1631.

Bröer A, Brookes N, Ganapathy V, Dimmer KS, Wagner CA, Lang F, Bröer S (1999) The astroglial ASCT2 amino acid transporter as a mediator of glutamine efflux. J Neurochem 73:2184–2194.

Bröer S, Brookes N (2001) Transfer of glutamine between astrocytes and neurons. J Neurochem 77:705–719.

Chairoungdua A, Kanai Y, Matsuo H, Inatomi J, Kim DK, Endou H (2001) Identification and characterization of a novel member of the heterodimeric amino acid transporter family presumed to be associated with an unknown heavy chain. J Biol Chem 276:49390–49399.

Chaudhry FA, Reimer RJ, Krizaj D, Barber D, Storm-Mathisen J, Copenhagen DR, Edwards RH (1999) Molecular analysis of system N suggests novel physiological roles in nitrogen metabolism and synaptic transmission. Cell 99:769–780.

Chaudhry FA, Schmitz D, Reimer RJ, Larsson P, Gray AT, Nicoll R, Kavanaugh M, Edwards RH (2002) Glutamine uptake by neurons: interaction of protons with system A transporters. J Neurosci 22:62–72.

Christensen HN (1990) Role of amino acid transport and countertransport in nutrition and metabolism. Physiol Rev 70:43–77.

Christensen HN, Liang M, Archer EG (1967) A distinct Na^+-requiring transport system for alanine, serine, cysteine, and similar amino acids. J Biol Chem 242:5237–5246.

de Koning TJ, Duran M, Dorland L, Gooskens R, Van Schaftingen E, Jaeken J, Blau N, Berger R, Poll-The BT (1998) Beneficial effects of L-serine and glycine in the management of seizures in 3-phosphoglycerate dehydrogenase deficiency. Ann Neurol 44:261–265.

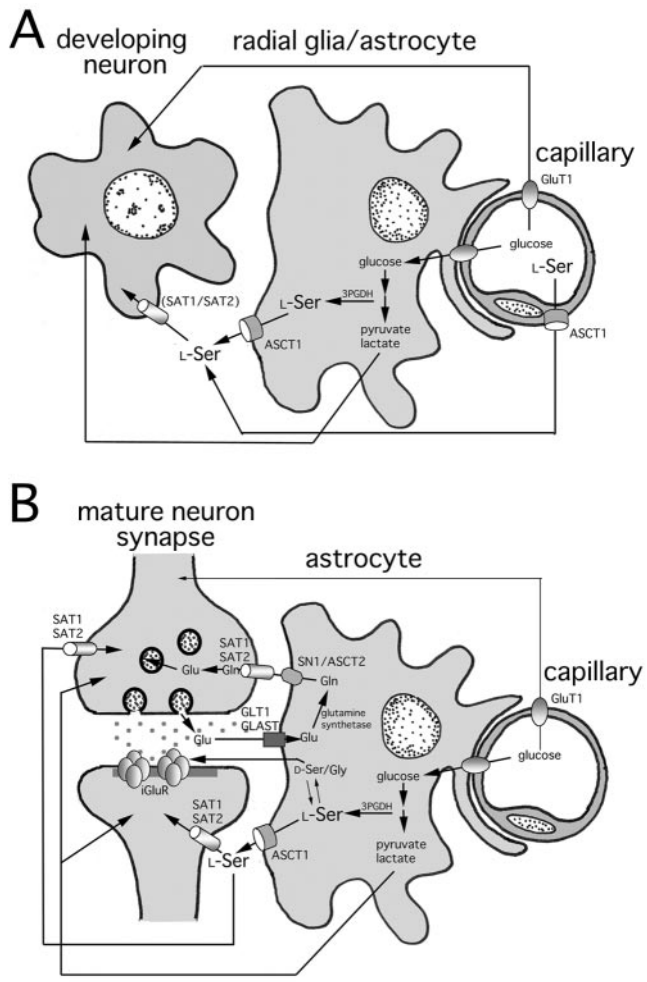

Figure 10. Schematic illustrations for ASCT1-mediated amino acid transport in the developing (*A*) and adult (*B*) brains. We incorporate our present finding on ASCT1 into prevailing schemes for the metabolic coupling among neuron (*synapse*), astrocyte, and capillary (Magistretti et al., 1999; Bröer and Brookes, 2001). In *B*, D-Ser and Gly (*D-Ser/Gly*) are shown as coagonists for the NMDA type of the ionotropic Glu receptor (*iGluR*). See Discussion.

de Koning TJ, Duran M, Van Maldergem L, Pineda M, Dorland L, Gooskens R, Jaeken J, Poll-The BT (2002) Congenital microcephaly and seizures due to 3-phosphoglycerate dehydrogenase deficiency: outcome of treatment with amino acids. J Inherit Metab Dis 25:119–125.

Doucette R (1991) PNS-CNS transitional zone of the first cranial nerve. J Comp Neurol 312:451–466.

Fukasawa Y, Segawa H, Kim JY, Chairoungdua A, Kim DK, Matsuo H, Cha SH, Endou H, Kanai Y (2000) Identification and characterization of a Na^+-independent neutral amino acid transporter that associates with the 4F2 heavy chain and exhibits substrate selectivity for small neutral D- and L-amino acids. J Biol Chem 275:9690–9698.

Furuya S, Tabata T, Mitoma J, Yamada K, Yamasaki M, Makino A, Yamamoto T, Watanabe M, Kano M, Hirabayashi Y (2000) L-Serine and glycine serve as major astroglia-derived trophic factors for cerebellar Purkinje neurons. Proc Natl Acad Sci USA 97:11528–11533.

Gu S, Roderick HL, Camacho P, Jiang JX (2000) Identification and characterization of an amino acid transporter expressed differentially in liver. Proc Natl Acad Sci USA 97:3230–3235.

Jaeken J, Detheux M, Van Maldergem L, Foulon M, Carchon H, Van Schaftingen E (1996) 3-Phosphoglycerate dehydrogenase deficiency: an inborn error of serine biosynthesis. Arch Dis Child 74:542–545.

Kekuda R, Prasad PD, Fei YJ, Torres-Zamorano V, Sinha S, Yang-Feng TL, Leibach FH, Ganapathy V (1996) Cloning of the sodium-dependent, broad-scope, neutral amino acid transporter B^0 from a human placental choriocarcinoma cell line. J Biol Chem 271:18657–18661.

Klomp LW, de Koning TJ, Malingre HE, van Beurden EA, Brink M, Opdam FL, Duran M, Jaeken J, Pineda M, van Maldergem L, Poll-The BT, van den Berg IE, Berger R (2000) Molecular characterization of 3-phosphoglycerate dehydrogenase deficiency: a neurometabolic disorder associated with reduced L-serine biosynthesis. Am J Hum Genet 67:1389–1399.

Lefauconnier JM, Trouve R (1983) Developmental changes in the pattern of amino acid transport at the blood-brain barrier in rats. Brain Res 282:175–182.

Lowry OH, Rosebrough NJ, Farr AL, Randall RJ (1951) Protein measurement with the folin phenol reagent. J Biol Chem 193:265–275.

Magistretti PJ, Pellerin L, Rothman DL, Shulman RG (1999) Energy on demand. Science 283:496–497.

Marin-Padilla M, Amieva MR (1989) Early neurogenesis of the mouse olfactory nerve: Golgi and electron microscopic studies. J Comp Neurol 288:339–352.

Matsuo H, Tsukada S, Nakata T, Chairoungdua A, Kim DK, Cha SH, Inatomi J, Yorifuji H, Fukuda J, Endou H, Kanai Y (2000) Expression of a system L neutral amino acid transporter at the blood-brain barrier. NeuroReport 11:3507–3511.

Mitoma J, Furuya S, Hirabayashi Y (1998) A novel metabolic communication between neurons and astrocytes: non-essential amino acid L-serine released from astrocytes is essential for developing hippocampal neurons. Neurosci Res 30:195–199.

Nakanishi S, Nakajima Y, Masu M, Ueda Y, Nakahara K, Watanabe D, Yamaguchi S, Kawabata S, Okada M (1998) Glutamate receptors: brain function and signal transduction. Brain Res Brain Res Rev 26:230–235.

Ramón-Cueto A (2000) Olfactory ensheathing glia transplantation into the injured spinal cord. Prog Brain Res 128:265–272.

Reimer RJ, Chaudhry FA, Gray AT, Edwards RH (2000) Amino acid transport system A resembles system N in sequence but differs in mechanism. Proc Natl Acad Sci USA 97:7715–7720.

Sánchez del Pino MM, Hawkins RA, Peterson DR (1992) Neutral amino acid transport by the blood-brain barrier: membrane vesicle studies. J Biol Chem 267:25951–25957.

Sánchez del Pino MM, Peterson DR, Hawkins RA (1995) Neutral amino acid transport characterization of isolated luminal and abluminal membranes of the blood–brain barrier. J Biol Chem 270:14913–14918.

Savoca R, Ziegler U, Sonderegger P (1995) Effects of L-serine on neurons in vitro. J Neurosci Methods 61:159–167.

Shafqat S, Tamarappoo BK, Kilberg MS, Puranam RS, McNamara JO, Guadano-Ferraz A, Fremeau Jr RT (1993) Cloning and expression of a novel Na^+-dependent neutral amino acid transporter structurally related to mammalian Na^+/glutamate cotransporters. J Biol Chem 268:15351–15355.

Shibata T, Yamada K, Watanabe M, Ikenaka K, Wada K, Tanaka K, Inoue Y (1997) Glutamate transporter GLAST is expressed in the radial glia–astrocyte lineage of developing mouse spinal cord. J Neurosci 17:9212–9219.

Snell K (1984) Enzymes of serine metabolism in normal, developing and neoplastic rat tissues. Adv Enzyme Regul 22:325–400.

Stryer L (1995) Biochemistry, Ed 4. New York: Freeman.

Utsunomiya-Tate N, Endou H, Kanai Y (1996) Cloning and functional characterization of a system ASC-like Na^+-dependent neutral amino acid transporter. J Biol Chem 271:14883–14890.

Varoqui H, Zhu H, Yao D, Ming H, Erickson JD (2000) Cloning and functional identification of a neuronal glutamine transporter. J Biol Chem 275:4049–4054.

Verleysdonk S, Hamprecht B (2000) Synthesis and release of L-serine by rat astroglia-rich primary cultures. Glia 30:19–26.

Wade LA, Brady HM (1981) Cysteine and cystine transport at the blood-brain barrier. J Neurochem 37:730–734.

Weiss MD, Derazi S, Kilberg MS, Anderson KJ (2001) Ontogeny and localization of the neutral amino acid transporter ASCT1 in rat brain. Brain Res Dev Brain Res 130:183–190.

Yamasaki M, Yamada K, Furuya S, Mitoma J, Hirabayashi Y, Watanabe M (2001) 3-Phosphoglycerate dehydrogenase, a key enzyme for L-serine biosynthesis, is preferentially expressed in the radial glia/astrocyte lineage and olfactory ensheathing glia in the mouse brain. J Neurosci 21:7691–7704.

Yao D, Mackenzie B, Ming H, Varoqui H, Zhu H, Hediger MA, Erickson JD (2000) A novel system A isoform mediating Na^+/neutral amino acid cotransport. J Biol Chem 275:22790–22797.

Yasuda E, Ma N, Semba R (2001) Immunohistochemical demonstration of L-serine distribution in the rat brain. NeuroReport 12:1027–1030.

Zerangue N, Kavanaugh MP (1996) ASCT-1 is a neutral amino acid exchanger with chloride channel activity. J Biol Chem 271:27991–27994.